J Mol Model (2003) 9:316–324
DOI 10.1007/s00894-003-0147-8

ORIGINAL PAPER

Marcin Król

Analysis of the effect of electrostatic energy truncation in molecular dynamics simulations of immunoglobulin G light chain dimer

Received: 5 December 2002 / Accepted: 12 June 2003 / Published online: 24 July 2003

Abstract Molecular dynamics (MD) simulations of immunoglobulin G (IgG) light chain dimer using particle mesh Ewald (PME) and cutoff methods of treating electrostatic interactions were performed. The results indicate that structural parameters (RMSD, radius of gyration, solvent accessible surface) are very similar for both schemes; however, PME simulation shows increased mobility of side chains. This leads to larger fluctuations in the distance between the monomers in the dimer molecule, and, as a consequence, results in decreased number of interactions across the dimer interface. The wall clock time of the simulations was also compared. It was shown that the PME method is approximately 30% faster than the cutoff method for the system studied on a single processor.

Keywords Molecular dynamics · Particle mesh Ewald · Long-range electrostatic interactions · Immunoglobulin G light chain dimer

Introduction

The treatment of long-range electrostatic interactions in molecular dynamics (MD) simulations of biologically important molecules has been the subject of several studies published over the last few years. [1, 2, 3] The influence of the treatment of long-range electrostatic interactions on the dynamic and structural properties of simulated systems has been shown to be substantial. On the other hand, it is often not possible to include interactions between all particles (atoms) present in the system, as the number of interactions is proportional to the square of the number of particles and becomes computationally very expensive even for medium-size biological systems. Therefore, one of the common ways to handle electrostatic interactions is to neglect them beyond a given cutoff radius. Different truncation schemes have been proposed [4] and tested in molecular dynamics simulations of proteins and nucleic acids. However, many researchers have pointed out that various cutoff schemes perform differently and sometimes significantly affect the simulated systems. Often found problems include lower stability of the simulation, [5] especially in the case of DNA and RNA molecules, [6] artificial stabilization of water molecules at the cutoff distance [7] leading to greater viscosity and a lower translational diffusion constant, [8] distorted water dipole–dipole spatial correlations [9] and large deviations of charged residues from the starting structure. [10] Among the cutoff schemes best results seem to be obtained with the force switching function model [4] where not the electrostatic energy but rather the force is switched to zero in the switch region.

In order to avoid shortcomings of a cutoff simulation, several ways to include long-range interactions have been proposed. [11, 12, 13] One of the most frequently used methods is the Ewald technique, [14] and its efficient and fast implementation—particle mesh Ewald [15] (PME) where the total electrostatic energy is split into direct and reciprocal Ewald sums and the latter is calculated with the use of a fast Fourier transform.

Several comparisons between cutoff and PME schemes have been published. However, these studies have been limited to pure water, [7, 16, 17] ions, [18] peptides, [9, 19, 20] small proteins [21, 22] and DNA. [6, 23] Therefore, it would be interesting to compare the performance of the PME and cutoff schemes when used in MD simulations of large, polymeric proteins. The presence of an interface between domains in a polymeric protein and electrostatic and hydrophobic interactions across the interface, which stabilize the whole molecule, constitute a stringent test for the method used. Inadequate treatment of electrostatic energy is likely to cause large

M. Król (✉)
Department of Bioinformatics
and Telemedicine Collegium Medicum,
Jagiellonian University,
Kopernika 17, 31-501 Kraków, Poland
e-mail: mykrol@cyf-kr.edu.pl
Tel.: +4812 4214057
Fax: +4812 4214057

conformational changes in the region of the interface, which are unlikely to be supported by experimental measurements.

Consequently, the immunoglobulin G (IgG) light chain dimer has been chosen for the present study. This large dimeric protein, consisting of 432 amino acids, 216 in each chain (amino acids 1–113 constitute variable domains (VLs) and 114–216 belong to constant domains (CLs)), has been extensively analyzed experimentally by our group. [24, 25, 26] It was shown that the protein forms complexes with Congo red. [27] Recently, the protein has been used as a model system to analyze transmission of immunological signals [28] and to test the performance of various implicit solvation models in molecular dynamics simulations. [29]

The aim of this work is to assess which electrostatic scheme gives better results in terms of structural and dynamic parameters and computational resources needed in molecular dynamics simulations of large dimeric proteins, such as IgG light chain dimer. The results of this work will be used to set up MD simulations of an IgG light chain dimer–Congo red complex.

In this work we evaluate the stability of the simulations by analyzing RMS distance (RMSD) time series, averaged over CA atoms, calculated relative to the starting structure, radius of gyration, total solvent accessible surface area, together with the contributions from charged (Lys, Arg, His, Asp, Glu), polar (Ser, Thr, Asn, Gln, Tyr, Cys) and hydrophobic (Gly, Ala, Val, Leu, Ile, Met, Pro, Phe, Trp) residues. RMSD values were calculated individually for each domain and for the whole molecule. Moreover, the number of interdomain nonbonding interactions is compared. In addition, we assess the dynamic behavior of the proteins by calculating RMS fluctuations (RMSFs) about the average structure and backbone order parameters. RMSFs were averaged over all nonhydrogen atoms for each residue. All coordinate frames were oriented with respect to the crystal structure prior to RMSF calculation. *B*-factors were converted into RMSFs according to the formula:

$$\mathrm{RMSF}_i = \sqrt{3B_i/8\pi^2}$$

Materials and methods

Simulation system

The crystal structure of immunoglobulin G (IgG) light chain dimer was obtained from the Protein Data Bank (PDB entry 4BJL). The resolution of the structure is 2.4 Å and the *R*-factor is 0.155. All hydrogens (param22) [30] were added to the PDB file by the HBUILD facility of CHARMM, [31] which resulted in 6,268 atoms. The initial structure was energy minimized by 150 steps with steepest descent (SD) and conjugate gradient (CG) methods. Only side chain atoms were allowed to move. After removal of the original steric clashes, the protein was immersed in a rectangular box of TIP3P water molecules. The position of the protein solute in the box was optimized by the Simulaid [32] program to yield the smallest possible box dimensions with the minimal primary atom—image atom distance set to 25 Å. As a result a rectangular box of 82.93 Å×70.51 Å×85.10 Å was created. The resulting system was then subjected to 150 steps of minimization (SD) and 29 ps of molecular dynamics (MD) simulation with all protein atoms kept fixed. Subsequently, the Genion [33] program was used to add eight Na^+ ions in order to construct a neutral simulation cell. Ions were placed in the region of low electrostatic potential in the space surrounding the protein. The system was equilibrated through 20 ps of constant volume MD at 300 K in which protein atoms were kept fixed. The final starting structure contained 6,268 protein atoms, 43,644 water atoms and eight Na^+ ions, which gave a total number of 49,920 atoms in the system.

Computational details

All simulations were performed using the CHARMM 27b2 program [31] with the param22 [30] all-atom force field. All bonds involving hydrogen atoms and the hydrogen–hydrogen distances in water were fixed using the SHAKE [34] algorithm. The time step was set to 2 fs. For the cutoff calculations, all nonbonding interactions were switched to zero at the cutoff distance of 12 Å. The force switch algorithm was used. [4] In the case of the PME calculation, the grid density was ~1 point/Å, κ=0.32 and sixth interpolation order was used. A direct space cutoff of 10 Å was used. Firstly, the systems were subjected to 9 ps of constant volume MD simulation, during which the temperature of the system was raised from 100 K to 300 K with the velocity rescaled every 0.2 ps. At 300 K, a 70-ps equilibration phase was started with the velocity rescaled every 0.2 ps during the first 20 ps. In the later stage of the equilibration, the velocity was rescaled only if the temperature of the system deviated more than 5 K from 300 K. At the end of the equilibration, the simulation energy and temperature of the systems were stable and no velocity rescaling was necessary for the last 20 ps. After equilibration, the systems were subjected to 1 ns of NPT-MD at 300 K and 100 kPa (0.987 atm) with the extended system. [35] The piston mass was set to 250.0 amu and 500.0 amu and parameter gamma to 25.0 ps^{-1} and 10.0 ps^{-1} for equilibration and production runs, respectively.

Results and discussion

It is very important that the methods employed sustain native-like conformations of the systems studied; therefore, in this section several parameters that assess the structural stability of both schemes in the course of the MD simulation are analyzed for the IgG light chain dimer molecule. Additionally, the dynamic behavior of the molecule is estimated. Furthermore, noncovalent interactions over the dimer interface and the interface are described and analyzed.

RMSD profiles for each domain separately and for the whole molecule were calculated to check the stability of each simulation. It should be noted that both chains (A and B) behave independently to a large extent and, as a consequence, constitute two partially independent simulation systems; therefore, calculation of RMSD for each domain is important, as it allows for checking if not only the whole molecule but also each domain is stable during simulations. On the other hand, the molecule is a proper system to examine treatment of noncovalent interactions between the monomers, which stabilize and maintain the dimer.

Noncovalent interactions across the dimer interface

The structure of the IgG light chain dimer is stabilized by a number of weak, nonbonding interactions: hydrogen bonds, van der Waals interactions and salt bridges. It would, therefore, be interesting to analyze the behavior of these interactions in the course of an MD simulation with both electrostatic schemes. It is important to point out that the interface between variable domains (variable interface) and the interface between constant domains (constant interface) differ from each other in the number of interactions and, consequently, they are analyzed separately.

Hydrogen bonds

There are four hydrogen bonds between the variable domains and 18 between the constant domains in the crystal structure of IgG light chain dimer. None of them are bridged by a water molecule. Figure 1 shows a time profile for a number of hydrogen bonds formed between variable domains and constant domains, respectively, without interactions via a water molecule. It is interesting to note that the number of hydrogen bonds in both models decreases to approximately 7 and 10 hydrogen bonds for PME and cutoff simulations in the case of the constant interface and to 1 and 2 hydrogen bonds in the case of the variable domain. This can be explained by the fact that protein hydrogen bond donors are involved in interactions with water molecules and less with the other polypeptide chain. Further analysis confirms this view, as some of the protein donors (such as Lys 133 and Lys 167) that were involved in hydrogen bonds in the crystal structure interact with water molecules. Figure 1 also shows the number of hydrogen bonds between the domains bridged by water molecules. The number of such interactions increases with respect to the X-ray structure, thus indicating that water molecule–protein interactions are stronger and occur more often during the simulation than during the crystallization process. However, the total number of hydrogen bonds in the course of the PME simulation is decreased compared to a cutoff run. This may suggest that hydrogen bonds are less stabilized in PME calculations. One probable reason is that side-chain mobility is increased in PME compared to the cutoff calculations. Another reason could be that the interface between monomers undergoes a larger conformational change in PME than cutoff simulations and the distance between monomers is increased.

Salt bridges

Salt bridges were analyzed based on the definition given by Barlow and Thorton [36] who recognize a salt bridge if a distance between centers of oppositely charged groups is lower than 4 Å. Based on this definition there are no salt bridges over the variable interface and one salt bridge

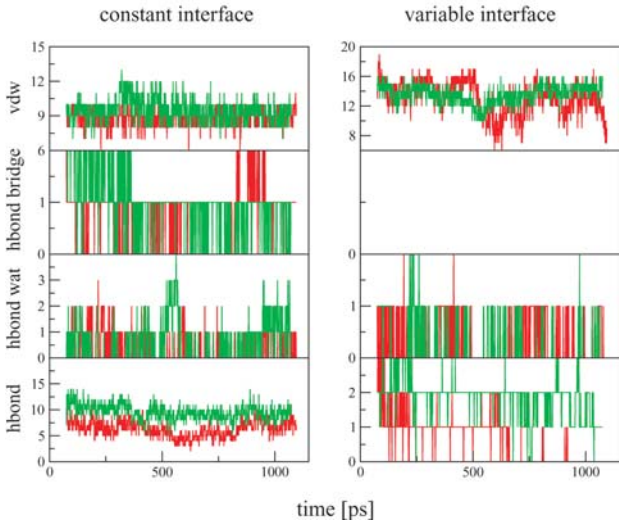

Fig. 1 Number of hydrogen bonds, bridged hydrogen bonds, salt bridges and van der Waals interactions across the dimer interface for both domains in PME (*red*) and cutoff (*green*) simulations

(formed by Glu 127 of chain A and Lys 424 of chain B) over the constant interface in the crystal structure. No salt bridges are formed in the course of the MD simulations over the variable interface and number of salt bridges over the constant interface is shown in Fig. 1. The salt bridge is well maintained in both models, which indicates that short-range electrostatic interactions are well sustained in both simulation protocols.

Van der Waals interactions

It is difficult to define a stringent criterion for van der Waals (vdW) interactions. In this work vdW interactions were recognized if two hydrophobic residues had their hydrophobic groups separated by less than 5 Å. This ensures that all interactions which contribute at least 1 kcal mol^{-1} to the stabilization energy are included. According to this definition there are 13 and 11 interactions across variable and constant interfaces in the starting structure, respectively. A plot showing a time profile of van der Waals contacts is shown in Fig. 1. It is interesting to note that number of vdW contacts for a variable domain cutoff simulation is held constant at approximately 14, while the number of contacts during PME calculations fluctuates strongly between 8 and 19. This may confirm higher mobility of the side chains at the dimer interface and larger conformational changes of the interface, signaled by the decreased number of hydrogen bonds. Moreover, the distance between two monomers in the course of the PME simulation may not be sustained and, as a consequence, the number of interactions across the dimer interface varies during PME calculations.

In order to assess stability and behavior of the whole dimer and verify the assumption that the distance between the monomers shows larger fluctuations in PME than in

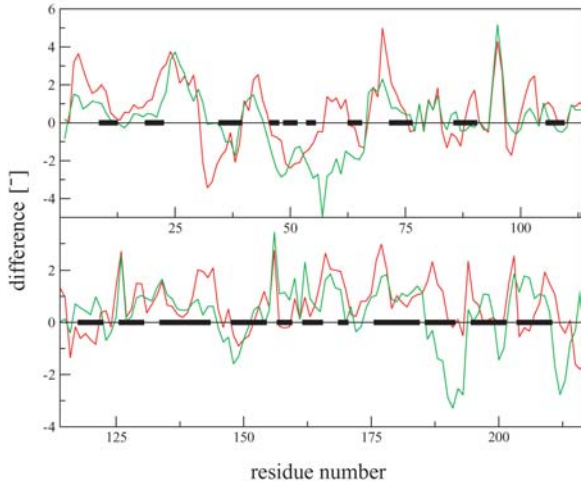

Fig. 2 Differences in CA–CA distances (Å) over the dimer interface between post-dynamics and crystal structures. *Red* line shows PME and *green* line shows cutoff results. *Thick* lines on the zero axes show stable secondary structures (see text). Upper part of the picture depicts distances in variable domain and lower in constant domain of IgG light chain dimer

cutoff simulations, the mutual orientation of two polypeptide chains constituting the dimer was monitored during MD simulations. Differences in CA–CA distances over the dimer interface between crystal and post-dynamics structures were calculated. They are shown in Fig. 2, for the constant and variable domains of light chain, respectively. Points above the 0 line indicate fragments in the dimer that are farther apart and points below 0 indicate fragments that are closer in post-dynamics structures compared to the crystal. Thick lines at the zero line indicate stable secondary structure fragments (β-structural and α-helical) calculated with the DSSP program [37] for both monomers in the crystal structure. To quantify the changes, several parameters were calculated and are given in Table 1: (1) average values of absolute distance differences (AADD) between the interdomain CA–CA distances in crystal and post-dynamics structures; (2) correlation coefficients between distances in crystal and post-dynamics structures; (3) number of distances that increased and decreased in simulations; (4) magnitude of the change. Overall, good agreement in the changes in the distance between monomers in cutoff and PME post-dynamics structures is seen for a variable domain. There is a large discrepancy for residues around amino acid 58, where monomers approach each other in cutoff calculations and draw away in PME calculations. This fragment, however, does not belong to a well-defined secondary structure region and may undergo conformational changes in the course of the dynamics simulation. For a constant domain, changes are also similar with differences around residue number 185, where two monomers draw away in PME and approach in cutoff simulations. The size of the approach and the fact that the fragment around residue 185 belongs to a well-defined secondary structure region indicate that a conformational change leading away from the native structure appears in cutoff simulation. No such change is found in the PME simulation. With the exception of the region around residue 185, the interface between the monomers behaves comparably in the two simulations and is not changed in the course of the MD run. This view is confirmed by data shown in Table 1. The average change in the distance between crystal and post-dynamics structures is about 1.1 Å for both electrostatic schemes and very high values of correlation coefficients calculated for interdomain distances in starting and post-dynamics structures indicate that the interface has been sustained in both simulations. The number of increased distances is greater in both simulations; however, the average increase is larger and average decrease smaller in the PME scheme, thus indicating that the interface has expanded slightly compared to starting and cutoff post-dynamics structures. This may explain the decrease in the number of hydrogen bonds observed in the PME simulation scheme.

RMSD

RMSD time profiles for the whole molecule are plotted in Fig. 3a and for all four domains in Fig. 3b. The stability of both calculations is excellent, with RMSD oscillating between 1 and 1.5 Å for all domains. No RMSD time series show any drift, thus indicating that conformational space around the crystal structure is a local minimum for both simulations. The PME calculation gives lower overall RMSD values in the case of the A monomer, while for the B monomer constant domain the opposite is true. However, the difference between RMSD values is low (less that 0.3 Å) and is on the order of the difference of the same method for two chains. RMSD profiles for the whole molecule are also relatively small, not exceeding 2.5 Å and their fluctuations are not the result of any changes in domain structure (stable and low RMSD for each domain), but changes in quaternary structure.

Table 1 Absolute value of average change in interdomain distances (AADD) between crystal and post-dynamics structures, correlation coefficient between interdomain distances in crystal and post-dynamics structures, number of increased and decreased distances together with the average changes for PME and cutoff calculations of IgG light chain dimer

	AADD (Å)	Correlation coefficient	No. of increased distances	Average increase (Å)	No. of decreased distances	Average decrease (Å)
PME	1.180	0.963	150	1.297	66	–0.915
Cutoff	1.075	0.962	136	1.027	88	–1.156

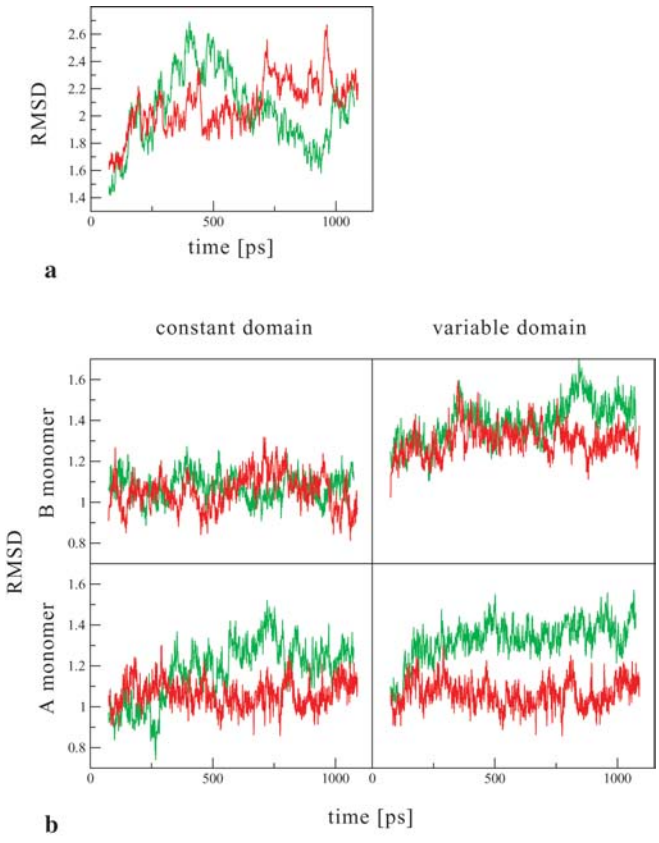

Fig. 3 **a** RMSD (Å) time profile calculated for the whole molecule; **b** RMSD (Å) time profile calculated for each domain separately. *Red* line depicts PME and *green* line depicts cutoff simulations

Nonetheless, moderate RMSD values for the whole molecule indicate that such changes are small.

Radius of gyration

Radius of gyration time profiles for both models together with the crystal value are shown in Fig. 4. Both models show a slight expansion of the structure compared to the starting structure. This is consistent with earlier studies of the PBC simulation protocol reported by Fox and Kollman. [5] After the initial expansion, both time profiles are relatively stable and fluctuate between 24.2 and 24.8 Å, with the PME values reaching the upper part of the interval, and cutoff values hitting the bottom of the interval. It is interesting to note that, at the end of the simulation, the radius of gyration for the cutoff scheme decreases rapidly. This decrease, however, does not seem to be a sudden structural rearrangement, as RMSD time profiles do not indicate that any such change is beginning to take place. More probably it is another fluctuation similar to the one observed around 500 ps.

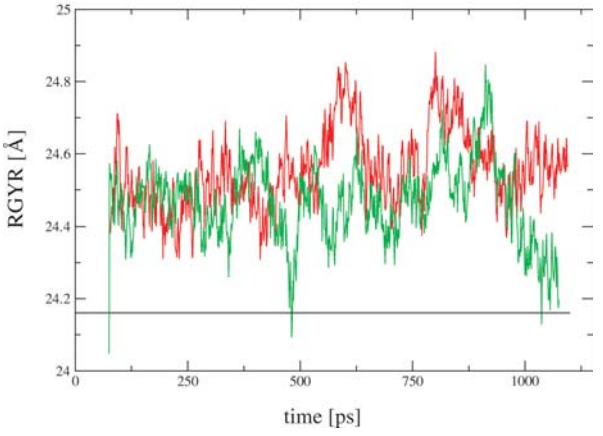

Fig. 4 Radius of gyration (Å) time profile for PME (*red*) and cutoff (*green*) simulations. *Black* line depicts crystal value

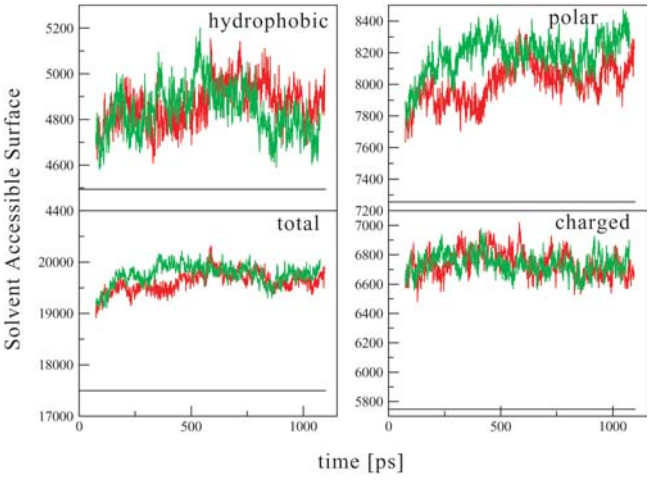

Fig. 5 Solvent accessible surface (Å^2) for all (total), hydrophobic, polar and charged residues for PME (*red*) and cutoff (*green*) simulations. *Black* line depicts crystal value

Solvent accessible surface (SAS)

SAS plots versus simulation time are shown in Fig. 5. Both simulation protocols yield higher total solvent accessible surface (TSAS) values compared to the starting structure due to the expansion of polar (PSAS) and hydrophobic (HSAS) residues contribution. The expansion ends at ~300 ps in the cutoff case and 600 ps in the case of the PME scheme. Both converge to the same value of about 20,000 Å^2. It seems that the structure in the cutoff simulation expands faster, as it does not "feel" the presence of other simulation cells. This is supported by the fact that in the case of the cutoff simulation, the contribution of polar residues to the solvent accessible surface increases during the first 200 ps, while the PSAS time profile for the PME calculation originally oscillates around the crystal value and increases at around 600 ps. It is interesting to note that there is a sudden, albeit temporary, expansion in the PME structure at 600 ps

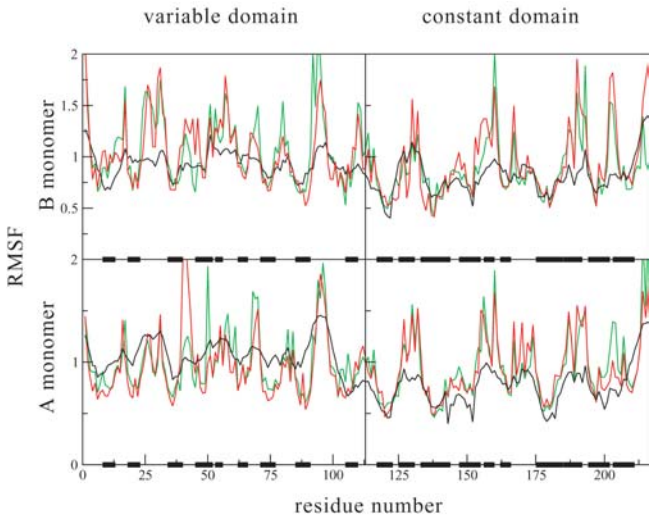

Fig. 6 RMS fluctuations (Å) about an average structure for PME (*red*) and cutoff (*green*) calculations. *Black* line shows RMS fluctuations derived from B-factors. *Thick*, horizontal lines show stable secondary structures

registered by the radius of gyration and the solvent accessible surface time profiles. Nonetheless, the last 400 ps of both simulations are stable in terms of solvent accessible surface and fluctuate around the same value of about 20,000 Å^2. Both total solvent accessible surface and contributions from polar, charged and hydrophobic residues expand to larger values compared to the crystal structure accessible surface. This expansion occurs in the heating and equilibration phases.

Dynamic parameters

Monitoring parameters that assess how well the starting structure is maintained is not enough to label a model good. It is also very important to check if low RMSD values are not the result of damping of important intramolecular motions or freezing out of molecular degrees of freedom. Therefore, RMSF profiles about the average structure were calculated and are shown in Fig. 6. Thick lines on the *x*-axis indicate stable secondary structure fragments (β-structural and α-helical) calculated with the DSSP program [37] for both monomers in the crystal structure. As seen from Fig. 6, the PME simulation protocol does not introduce any damping compared to the cutoff scheme, showing similar atomic fluctuations for all domains. Both simulation protocols yield average RMSF values similar to crystal-derived ones (given in Table 2), which gives evidence that neither of the methods damp internal intramolecular motions and allow the protein to sample conformational space about the local minimum defined by the crystal structure freely. Generally, PME and cutoff fluctuations correlate much better with each other than with experimental B-factors (correlation coefficients are given in Table 2). There are, however, fragments where differences between PME and cutoff fluctuations are profound, e.g. around residues 37–45, 75–86 and 90–100 of the A monomer and 63–75 and 165–175 of the B monomer. While the differences in the A monomer occur in regions without ordered secondary structure and, therefore, are of minor importance, the divergence in the B monomer occurs in both cases for fragments with well-defined secondary structure. This indicates that not only loops but also β-strands (IgG light chain dimer is a β-structural protein) fluctuate differently in the two simulation schemes. A comparison between calculated and crystal-derived fluctuations reveals a moderate correlation. However, general trends are well reproduced and minima overlap very well. This shows that fragments with low mobility in the crystal also show limited fluctuations in MD simulations. It is interesting to point out that low-fluctuating fragments belong to well-defined secondary structures (Fig. 6), which usually tend to have lower mobility than loop and random coil regions. Moreover, it should be noted that the protein molecule studied is large and other researchers [38, 39] have reported similar correlation coefficients between calculated and experimentally derived fluctuations for smaller proteins.

Another way of assessing the dynamic behavior of the protein is to calculate N–H backbone order parameters as asymptotic values of the autocorrelation function of the unit vector in the direction of the N–H bond. These order parameters were calculated and are shown in Fig. 7. Thick horizontal lines show stable secondary structure fragments. A large discrepancy between the two protocols for residues 35–45 of the A monomer is sustained, thus indicating that the whole polypeptide chain behaves differently in this region. As far as the B monomer is concerned, a large divergence occurs for residues 33, 50 and ~100 for a variable domain and 145, 160, and 200 for a constant domain. It is also interesting to point out that, even though RMSF plots for A and B differ, thus supporting the statement mentioned above that the two dimers behave independently to a large degree, closer analysis of backbone order parameters reveals that backbone motions are similar among monomers, especially for

Table 2 RMSFs (Å) for all heavy atoms for IgG light chain dimer molecule without N-and C-terminal residues of each chain

	Average RMSF (Å)	Correlation coefficient vs. experimental	Correlation coefficient vs. PME	Correlation coefficient vs. cutoff
Experimental	0.90	1	0.52	0.55
PME	0.98	0.52	1	0.80
Cutoff	0.97	0.55	0.80	1

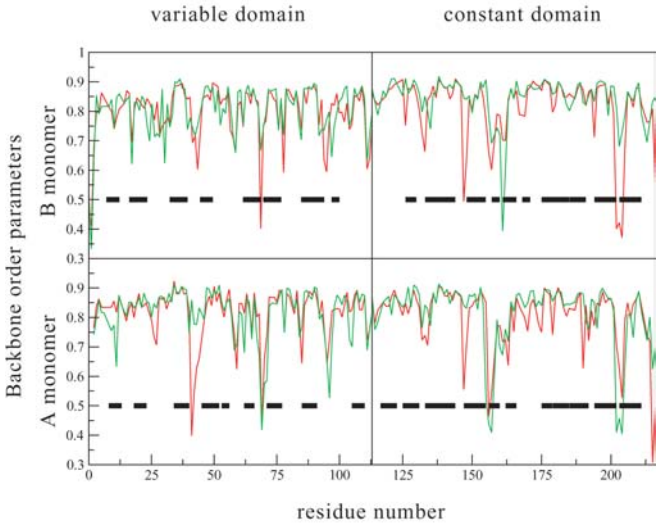

Fig. 7 Backbone order parameters for PME (*red*) and cutoff (*green*) calculations. *Thick*, horizontal lines show stable secondary structures

the constant domain, and differences in RMSF plots originate from dissimilar mobility of side chains. It is also important to state that all differences in backbone order parameters occur in fragments without stable secondary structure. Mobility of β-strands is low in both simulations, which indicates that stability of these fragments would be sustained even in much longer simulations.

Unfortunately, the IgG light chain dimer has not been studied by means of NMR and, as a consequence, no experimental backbone order parameters could be found. It would be of great interest to compare experimental data derived from analysis of the protein in solution, as it would be possible to check if backbone order parameters obtained from the simulations correlate better with experimentally derived ones than RMS fluctuations.

Crystal packing interactions

It could be pointed out that larger differences in post-dynamics and crystal structures may result from the lack of crystal packing forces in the MD simulation. Moreover, lack of these forces may increase atomic fluctuations measured by the RMSF. Therefore, crystal packing in the elementary cell was created with the program XPAND [40] and is shown in Fig. 8. Intermolecular close contacts were recognized if CA–CA distance between different molecules was shorter than 10 Å. Based on this definition, fragments interacting with other molecules in the crystal cell are identified. In the case of the A monomer, residues 126–132 and 215–216 and in case of B monomer residues 23–26, 30, 67–71, 119, 129–133, 156–162, 185–194 and 196–215 are involved in crystal contacts. If one compares these fragments with regions of large changes in interdomain distances (Fig. 2), one sees that there is no obvious correlation between them; however, significant changes in interdomain distances for the C-terminal fragment occur in the region involved in intermolecular contacts in the crystal. Other such regions include fragments around residue 30 (large interdomain distance difference for cutoff simulation), residue 70 (large interdomain distance difference for PME simulation) and residue 155. On the other hand, there are regions with large interdomain distance difference, which are not involved in crystal contacts (e.g. fragments 50–60 and around residue 95).

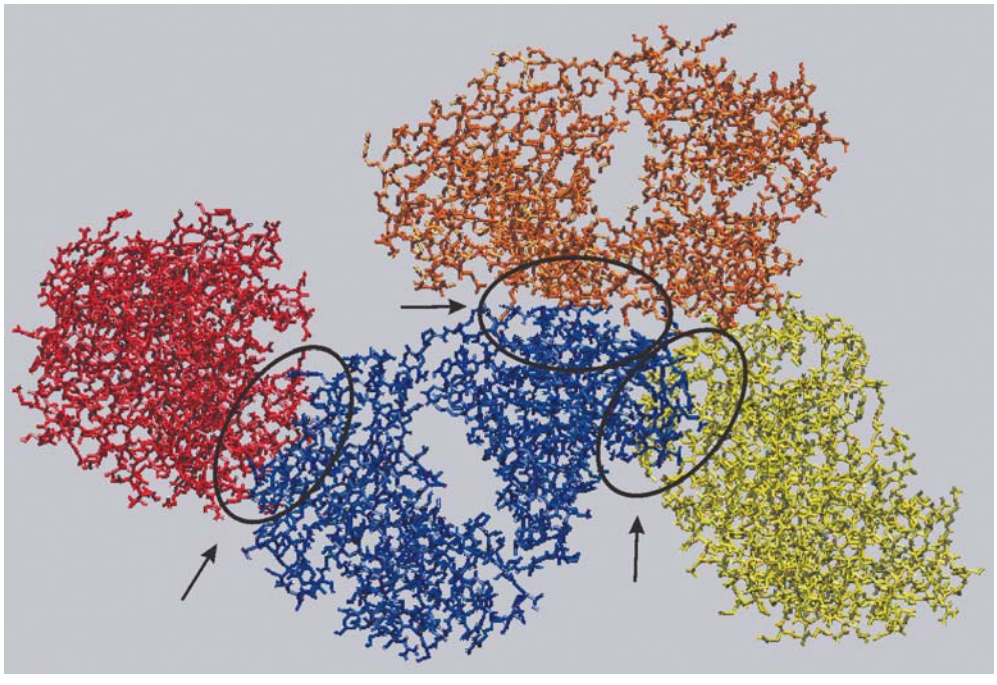

Fig. 8 Crystal cell packing for IgG light chain dimer (4bjl) molecule generated with XPAND program. Regions of intermolecular contacts are indicated

Comparison of fragments engaged in crystal contacts with highly fluctuating regions (Fig. 6) reveals that, although not all residues with large RMS fluctuations are involved in crystal contacts, the opposite statement is true—virtually all amino acids that form intermolecular contacts have large RMSF values.

These observations indicate that lack of crystal packing forces does not have a large impact on a simulated protein structure; however, it influences dynamic and structural parameters to a certain extent and molecular dynamics simulations in a crystal environment would be necessary to investigate this problem further.

CPU benchmark

It was shown in early papers on the Ewald technique that the method is very slow compared to cutoff simulations. However, with the advent of the PME method, the difference in CPU between reasonable cutoff (at least 12 Å) and PME was shown to be negligible. [8] To verify this point we have compared wall clock time of a 50-ps MD simulation for the cutoff and PME methods on a single processor AMD XP 1,600 MHz. The results are 76.38 h for PME and 118.42 h for cutoff. These results show that the modern PME method is, in theory, faster than the cutoff simulation. However, in practice when MD simulations are performed on PC clusters this time advantage of the PME method diminishes as this method parallelizes worse than cutoff calculations. This is, however, highly dependent on both hardware and software used. [41]

Conclusions

The aim of this work is to investigate the performance of two common schemes for treating electrostatic interactions in MD simulations of a large, dimeric protein molecule. The study shows that both methods perform comparably in terms of stability of the calculations. RMSD, radius of gyration and solvent accessible surface time series do not show any significant drift and differences in results for the two methods are within the difference of the same method for two monomers (RMSD). This is consistent with an earlier study on DNA by Norberg and Nilsson. [23] On the other hand, the two methods produce different results (to some extent) in terms of fluctuations monitored by RMSF plots. However, closer analysis and calculation of backbone order parameters shows that backbone mobility is sustained in both simulation schemes and that the PME model produces similar fluctuations of side chain atoms compared to cutoff simulations. This contradicts earlier work by Fox and Kollman [5] and Saito [10] who showed that cutoff simulations yield higher RMSF values. However, this may be attributed to a lower overall stability of the cutoff simulations, as the RMSD for the cutoff method was much higher in both aforementioned papers compared to PME. On the other hand, results presented in this paper are consistent with the paper by York et al. [21] who showed that, for crystal MD simulations, RMSF values derived from the PME scheme are approximately 10% higher than those obtained from cutoff calculations. On the whole, increased mobility of side chains is desirable as it proves that no damping of internal degrees of freedom takes place provided that RMSD values are low, which is achieved in simulations presented in this paper.

As wall clock time of the PME simulation is 30% lower than for the cutoff simulation, it is apparent that the former will be the method of choice in subsequent molecular dynamics simulations of the IgG light chain dimer. However, it should be noted that carefully chosen cutoff protocol and cutoff distance does not lead to large deviations in the case of MD simulations of the system studied.

Acknowledgement The author would like to thank Prof. Irena Roterman for her suggestions, comments and support of this study.

This work was supported by the Polish State Committee for Scientific Research (grant 4 T11F 015 22). Calculations were partially performed on SGI2800 high performance computer at Academic Computer Centre of Stanislaw Staszic University of Mining and Metallurgy in Kraków, Poland (grant KBN/SGI_ORIGIN_2000/UJ/106/1998).

References

1. Hummer G, Pratt LR, Garcia AE (1998) J Phys Chem A 102:7885–7895
2. Darden T, York D, Pedersen L (1993) J Chem Phys 98:10089–10092
3. Luty BA, van Gunsteren WF (1996) J Phys Chem 100:2581–2587
4. Steinbach PJ, Brooks BR (1994) J Comput Chem 15:667–683
5. Fox T, Kollman PA (1996) Proteins: Struct, Funct, Genet 25:315–334
6. Cheatham TE, Miller JL, Fox T, Darden TA, Kollman PA (1995) J Am Chem Soc 117:4193–4194
7. Mark P, Nilsson L (2002) J Comput Chem 23:1211–1219
8. Feller SE, Pastor RW, Rojnuckarin A, Bogusz S, Brooks BR (1996) J Phys Chem 100:17011–17020
9. Smith PE, Pettitt BM (1991) J Chem Phys 95:8430–8441
10. Saito M (1994) J Chem Phys 101:4055–4061
11. Forester T, Smith W (1994) Mol Simul 13:195–204
12. Zichi DA (1995) J Am Chem Soc 117:2957–2969
13. Shimada J, Kaneko H, Takada T (1994) J Comput Chem 15:28–43
14. Perram JW, Petersen HG, DeLeeuw (1988) Mol Phys 65:875–893
15. Essman U, Perera L, Berkowitz ML, Darden T, Lee H, Pedersen LG (1995) J Chem Phys 103:8577–8593
16. Levitt M, Hirshberg M, Sharon R, Laidig KE, Dagett V (1997) J Phys Chem B 101:5051–5061
17. van der Spoel D, van Maaren PJ, Berendsen HJC (1998) J Chem Phys 108:10220–10230
18. Perrera L, Essman U, Berkowitz ML (1995) J Chem Phys 102:450–456
19. Boresch S, Steinhauser O (1999) J Chem Phys 111:8271–8274
20. Weber W, Hünenberger PH, McCammon JA (2000) J Phys Chem B 104:3668–3675
21. York DM, Darden TA, Pedersen LG (1993) J Chem Phys 99:8345–8348

22. de Souza NO, Orstein RL (1999) J Biomol Struct Dyn 16:1205–1218
23. Norberg J, Nilsson L (2000) Biophys J 79:1537–1553
24. Roterman I, Rybarska J, Konieczny L, Skowronek M, Stopa B, Piekarska B, Bakalarski G (1998) Comput Chem 22:61–70
25. Konieczny L, Piekarska B, Rybarska J, Skowronek M, Stopa B, Tabor B, Dąbroś W, Pawlicki R, Roterman I (1997) Folia Histochem Cytobiol 35:203–210
26. Piekarska B, Konieczny L, Rybarska J, Stopa B, Zemanek G, Szneler E, Król M, Nowak M, Roterman I (2001) Biopolymers 59:446–456
27. Ward LD, Timashew SN (1994) Biochemistry 33:11891–11899
28. Król M, Roterman I, Piekarska B, Konieczny L, Rybarska B, Stopa B (2003) Biopolymers 69:189–200
29. Król M (2003) J Comput Chem 24:531–546
30. MacKerell Jr AD, Bashford D, Bellot M, Dunbrack Jr RL, Evenseck JD, Field MJ, Fischer S, Gao J, Guo H, Ha S, Joseph-McCarthy D, Kuchnir L, Kuczera K, Lau FTK, Mattos C, Michnick S, Ngo T, Nguyen DT, Prodhom B, Reiher III WE, Roux B, Schlenkrich M, Smith JC, Stote R, Straub J, Watanabe M, Wiorkiewicz-Kuczera J, Yin D, Karplus M (1998) J Phys Chem B 102:3586–3616
31. Brooks B, Bruccoleri R, Olafson B, States D, Swaminathan S, Karplus M (1983) J Comput Chem 4:187–217
32. Mezei MJ (1997) J Comput Chem 18:812–815
33. Lindahl E, Hess B, van der Spoel D (2001) J Mol Mod 7:306–317
34. Ryckaert J, Ciccotti G, Berendsen HJ (1977) J Comput Phys 23:327–341
35. Feller SE, Zhang Y, Pastor RW, Brooks BR (1995) J Chem Phys 103:4613–4621
36. Barlow DJ, Thornton JM (1983) J Mol Biol 168:867–885
37. Kabsch W, Sander C (1983) Biopolymers 22:2577–2637; PMID: 6667333; UI: 84128824
38. Elofsson A, Nilsson L (1993) J Mol Biol 233:766–780
39. Garemyr R, Elofsson A (1999) Proteins: Struct, Funct, Genet 37:417–428
40. Kleywegt GJ, unpublished program. Uppsala University, Uppsala, Sweden
41. Taufer M, Perathoner E, Cavalli A, Caflisch A, Stricker T (2002) Proc of IPDPS 2002, IEEE/ACM International Parallel and Distributed Processing Symposium, Fort Lauterdale, Fla., USA